J Sol-Gel Sci Technol (2014) 71:501–513
DOI 10.1007/s10971-014-3398-1

ORIGINAL PAPER

The sol–gel approach as a method of synthesis of $xMgO{\cdot}ySiO_2$ powder with defined physicochemical properties including crystalline structure

Filip Ciesielczyk · Milena Przybysz · Jakub Zdarta · Adam Piasecki · Dominik Paukszta · Teofil Jesionowski

Received: 30 September 2013 / Accepted: 9 May 2014 / Published online: 23 May 2014

Abstract The physicochemical properties of synthetic powders depend strongly on the method of their preparation. The present work concerns the use of the sol–gel method to prepare $xMgO{\cdot}ySiO_2$ powders with defined physicochemical and structural properties. An important objective was to determine how the basic process parameters (including the type and concentration of the reactants) influence the physicochemical properties of the resulting material. To obtain a synthetic powders, organic precursors of magnesium (magnesium ethoxide), and silicon (tetraethoxysilane) were used. Selected products were subjected to calcination to identify the crystalline structure of the powders and to determine the impact of the proposed method of preparation on this parameter. This aspect of the research will significantly improve the range of application of the manufactured products. The powders obtained by the proposed method were thoroughly analyzed in terms of chemical composition, crystalline structure, morphology and nature of dispersion, parameters of porous structure, and thermal as well as electrokinetic properties. The sol–gel process proved very effective in the synthesis of highly active powders, as evidenced by the very high values obtained for the products' surface area. It was also confirmed that the physicochemical parameters are strongly dependent on the mass ratio of the reactants and on the method of final treatment of the precipitates.

Keywords $xMgO{\cdot}ySiO_2$ powder · Sol–gel method · Chemical composition · Crystalline and porous structure

1 Introduction

Recent years have seen a noticeable rapid development of technologies and methods for the synthesis of inorganic powders, which are used in various industries (such as the ceramics, pharmaceuticals, food, cosmetics and construction industries). Among the many common techniques, one that is quite widely used is the sol–gel method [1, 2].

The sol–gel method is efficient in economic terms for the preparation of new synthetic powders with suitable physicochemical properties. The efficiency of the sol–gel process is affected by several parameters, including temperature, pH, amount and type of solvent used, type of catalyst and metal precursor, as well as the concentration of reagents [3–5].

The sol–gel method can be used for the synthesis of a large number of compounds, including hybrid powders, nanocomposites, nanopowders, and many others [6–10]. Due to the versatility and the flexibility of its process parameters, it can be used in many areas of science and industry, including medicine and dentistry. Deposition of thin film layers on glass, ceramic and metal is one of the most important applications of the sol–gel process [11]. The single or multiple oxide coatings obtained by this method are used on a large scale, and in terms of

Electronic supplementary material The online version of this article (doi:10.1007/s10971-014-3398-1) contains supplementary material, which is available to authorized users.

F. Ciesielczyk (✉) · M. Przybysz · J. Zdarta · D. Paukszta · T. Jesionowski
Faculty of Chemical Technology, Institute of Chemical Technology and Engineering, Poznan University of Technology, M. Sklodowskiej-Curie 2, 60965 Poznan, Poland
e-mail: Filip.Ciesielczyk@put.poznan.pl

A. Piasecki
Faculty of Mechanical Engineering and Management, Institute of Materials Science and Engineering, Poznan University of Technology, Jana Pawla II 24, 60965 Poznan, Poland

production costs are much cheaper than coatings prepared by other commonly used methods. In addition, the sol–gel method ensures the high purity of the products and the possibility of mixing organic and inorganic components on a nanometric scale. The process usually takes place at low temperature and in mild reaction conditions, which permits, for example, the trapping of molecules such as enzymes or proteins, which have low thermal and chemical stability [12].

The physicochemical properties of different powders significantly depend on the method of their preparation and heat treatment, which in many cases is the final step of the process. Synthetic powders are products of reaction carried out between precursors of different metals. However, hydrated mixed oxides can be obtained in hydro- or solvothermal conditions [13–15].

Production of this type of powders, according to the assumptions of the sol–gel process, involves hydrolysis of the organic metal precursor, such as magnesium alkoxide, in the presence of acid or base, followed by a polycondensation reaction. It has been shown that the process of hydrolysis strictly depends on the pH of the solution and the nature of the catalyst ($HCI > CH_3COOH > H_2C_2O_4 > H_2O > NH_4OH$) [16]. The hydrolysis reaction may be carried out in an acidic environment, and polycondensation in a basic medium [17, 18]. The sol–gel technique allows the use of different metal precursors, because the hydrolysis process is controlled by changing the pH of the reaction medium. The uniformity of the resulting gel also depends on such parameters as the solubility and order of dosing of the reactants, and the temperature and pH of the reaction. Moreover, in recent years, increasing interest in and demand for nanomaterials has been observed, especially in industrial applications. The quality of these products is largely dependent on their particle size, which can be designed precisely in the sol–gel process [19–21].

Very often the sol–gel method is used for the preparation of hybrid materials. The powders thus obtained, subjected to a calcination process, in many cases exhibit interesting crystalline structures with a broad spectrum of application [22–26].

The powders prepared based on the sol–gel method confirm its efficiency and versatility, and in addition are characterized by specific properties and can be used in many advanced technologies [27–30]. Bayala et al. [27] described the possibility of obtaining hybrid materials based on NiO (NiO·ZnO, NiO·CuO, NiO·MgO) which offer high thermal stability and can be used as catalysts. The authors proved that the selection of appropriate reactants and controlling the parameters of the sol–gel process determine the type of the materials and its physicochemical as well as useful properties. In turn, using titanium tetraisopropoxide (TTIP) and tetraethoxysilane (TEOS), it is possible, under appropriate process conditions, to obtain a hybrid $TiO_2{\cdot}SiO_2$ powders with specific optical properties for advanced manufacturing technology [28]. A study of the same materials ($TiO_2{\cdot}SiO_2$) is presented by Aguado et al. [29]. These authors confirmed that the selection of the parameters of the sol–gel process plays an important role in the preparation of powders with a suitable texture, crystalline structure and appropriate degree of incorporation of TiO_2. It also appears that, by controlling the weight ratio of the reagents, it is possible to obtain such materials as $TiO_2{\cdot}SiO_2$, $ZnO{\cdot}TiO_2$, $Al_2O_3{\cdot}TiO_2$ with different contents of the particular oxides, which has a decisive impact on the physicochemical properties of the final product [30]. The surface area of the systems was found to increase with increasing content of SiO_2. In addition, the activity of the precipitated powders increased with the temperature of final treatment, but only up to 700 °C, to avoid obtaining the rutile form of TiO_2.

With regard to the dynamic development of industry and the continuing need for new multifunctional materials, an attempt was made here to produce a novel $xMgO{\cdot}ySiO_2$ powder with defined physicochemical properties, including specified crystalline and porous structure. The materials obtained by the sol–gel method may serve as a new group of functional adsorbents or catalysts.

2 Experimental

2.1 Materials

The $xMgO{\cdot}ySiO_2$ powders were prepared by the sol–gel process using magnesium ethoxide as the organic precursor of magnesium. The process was carried out in a three-necked flask, to which in the first stage were added a certain amount of magnesium ethoxide and 100 cm^3 of methyl alcohol, which was used as the solvent. The whole mixture was stirred for 15 min, and then, using a peristaltic pump in a fixed sequence (three variants), the base catalyst—25 % ammonia, and the silicon precursor—TEOS were introduced.

The quantities of reagents were chosen so that the weight ratio of TEOS:magnesium precursor:NH_4OH in the different variants was 1.5:1:0.5 (samples labeled as MP 1.1–1.3), 1.5:1:0.25 (samples labeled as MP 3.1–3.3), 1:1:0.5 (samples labeled as MP 2.1–2.3) and 1:1:0.25 (samples labeled as MP 4.1–4.3). In this reaction system, ammonia acts as a catalyst of the gelation process as well as allows to control condensation rate. Two different amounts of this factor for the particular variants of the process were used, and a main objective was to determine the effect of its addition on the effectiveness of the precipitation of the product—the addition of NH_4OH affects the nucleation and growth of particles in the reaction

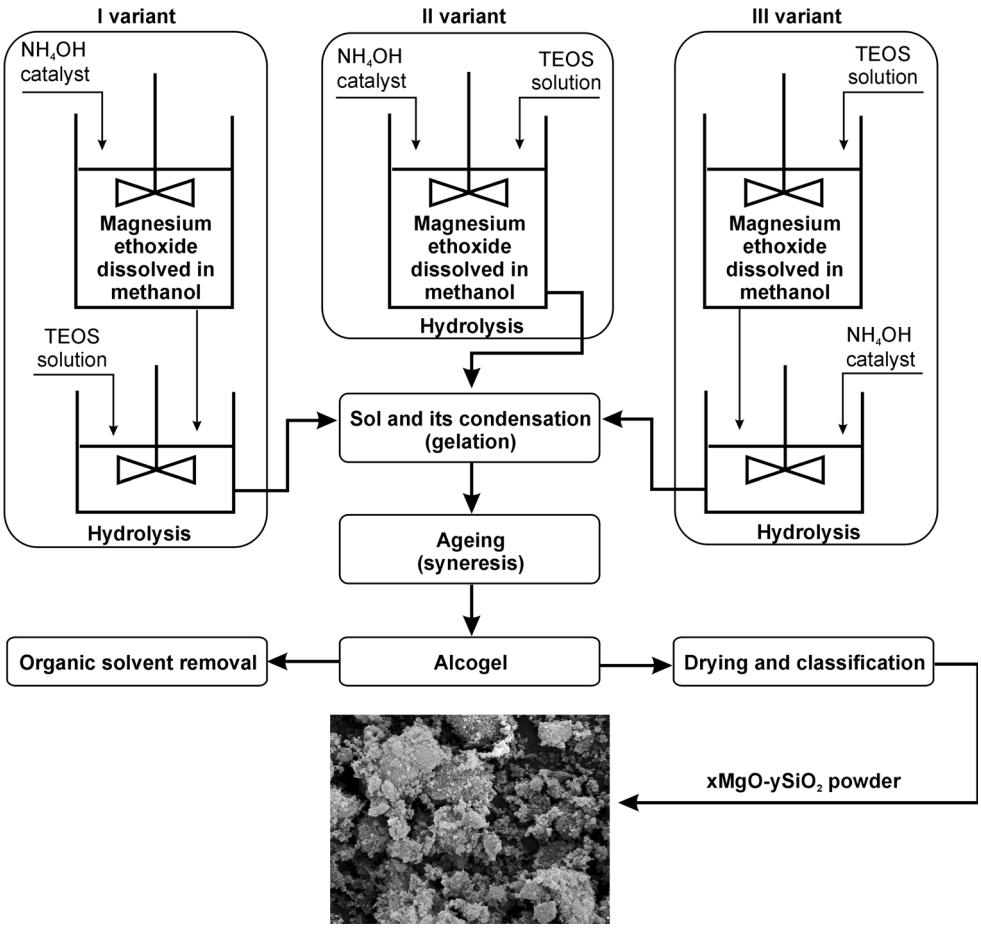

Fig. 1 Methodology of precipitation of $xMgO{\cdot}ySiO_2$ powders via the sol–gel method

system and can only result in their morphology, shape and porosity. The resulting system was stirred for 45 min using a high-speed stirrer (1,000 rpm) (IKA Werke GmbH). The synthesis was carried out at room temperature. The product obtained, in the form of alcogel, was placed in a vacuum evaporator to remove the solvent (methanol) and ammonia. The product in the form of granules was dried at 105 °C for 24 h. After the drying process the powder was classified and subjected to thorough physicochemical analysis. Selected products underwent calcination (at 1,000 °C for 2 h) to identify and evaluate the crystalline structure. A diagram of the process is shown in Fig. 1.

2.2 Evaluation of physicochemical properties of $xMgO{\cdot}ySiO_2$ powders

To confirm the effectiveness of the process, the chemical composition of synthetic materials was analyzed using atomic absorption spectrometry (AAS), with the use of a Hitachi spectrometer (content of Mg) and gravimetric method (content of SiO_2 and moisture). To perform this analysis 1 g of resulting powder, both subjected and not subjected to calcination, was leached in the $HCl:H_2O$ (1:1) solution during 1 h. After that time, whole mixture was filtrated—sediment was dried and subjected to gravimetric analysis to evaluate SiO_2 content, on the other hand the filtrate was subjected to AAS analysis to evaluate Mg content. The moisture content was determined by drying the initial samples at 105 °C for 2 h. Additionally to support those results the surface composition of prepared powder materials was analyzed using energy dispersive X-ray spectroscopy (EDS), with the use of a Princeton Gamma-Tech unit with a prism digital spectrometer. The calcinates of $xMgO{\cdot}ySiO_2$ powders also underwent crystalline structure determination using the WAXS method. The results were analyzed using X-Rayan software. Diffraction patterns were taken using a TUR-M62 horizontal diffractometer equipped with an HZG-3 type goniometer. The dispersive characteristics, morphology and microstructure of the products were analyzed using a Zeiss EVO40 scanning electron microscope. The observations enabled evaluation of the degree of dispersion, the structure of particles and their tendency towards aggregation or agglomeration. Using a Zetasizer Nano ZS (based on the non-invasive back scattering light method) it was possible to measure the electrophoretic mobility using laser Doppler

Table 1 Chemical composition of $xMgO{\cdot}ySiO_2$ powders obtained via sol–gel method

Element	Magnesium content from AAS analysis (mg/dm^3)					
	MP 1.1	MP 1.2	MP 1.3	MP 2.1	MP 2.2	MP 2.3
	TEOS:magnesium ethoxide:NH_4OH mass ratio 1.5:1:0.5			TEOS:magnesium ethoxide:NH_4OH mass ratio 1:1:0.5		
Mg^{2+}	1,680	1,520	1,410	2,310	2,060	2,040
$Mg^{2+}_{Average}$		1,537			2,137	
	MP 3.1	MP 3.2	MP 3.3	MP 4.1	MP 4.2	MP 4.3
	TEOS:magnesium ethoxide:NH_4OH mass ratio 1.5:1:0.25			TEOS:magnesium ethoxide:NH_4OH mass ratio 1:1:0.25		
Mg^{2+}	1,660	1,960	1,520	2,380	2,450	1,970
$Mg^{2+}_{Average}$		1,713			2,267	
Element	Silica and moisture content from gravimetric analysis (mas.%)					
	MP 1.1	MP 1.2	MP 1.3	MP 2.1	MP 2.2	MP 2.3
SiO_2	59.8	57.8	62.1	54.6	57.7	59.6
$SiO_{2Average}$		59.9			57.3	
H_2O	12.8	11.9	10.7	13.6	12.5	12.3
$H_2O_{Average}$		11.8			12.8	
	MP 3.1	MP 3.2	MP 3.3	MP 4.1	MP 4.2	MP 4.3
SiO_2	58.3	58.2	63.1	57.2	55.6	59.0
$SiO_{2Average}$		59.9			57.3	
H_2O	11.9	12.7	10.1	12.3	13.5	11.7
$H_2O_{Average}$		11.6			12.5	
Element	Mass contribution from EDS analysis (%)					
	MP 1.1	MP 1.2	MP 1.3	MP 2.1	MP 2.2	MP 2.3
Mg	17.9	16.6	15.4	24.7	22.8	21.5
$Mg_{Average}$		16.6			23.0	
Si	27.4	24.5	34.2	18.3	24.6	27.2
$Si_{Average}$		28.7			23.4	
O	54.7	58.9	50.4	57.1	52.6	51.3
$O_{Average}$		54.7			53.7	
	MP 3.1	MP 3.2	MP 3.3	MP 4.1	MP 4.2	MP 4.3
Mg	19.4	22.1	17.2	24.9	24.7	21.9
$Mg_{Average}$		19.6			23.7	
Si	24.5	27.5	32.7	22.7	22.9	26.0
$Si_{Average}$		28.2			23.9	
O	56.1	50.4	50.1	52.4	52.3	52.1
$O_{Average}$		52.2			52.3	

velocimetry (LDV), and indirectly the zeta potential (the Zetasizer Nano ZS software provides the ability to convert electrophoretic mobility values to zeta potential based on the Henry equation). The electrokinetic potential was measured over the whole pH range in the presence of 0.001 M NaCl electrolyte, which made it possible to determine the electrokinetic curves. The hybrid materials were also subjected to thermal stability analysis with the use of an STA449F3 apparatus (Netzsch GmbH). The tests were carried out in a nitrogen atmosphere, with the temperature varying over a range of 30–1,000 °C. The surface area A_{BET} (BET method) was calculated based on data measured by low-temperature adsorption of nitrogen. The isotherms of nitrogen adsorption/desorption were measured at −196 °C using an ASAP 2020 apparatus (Micromeritics Instrument Co.). Taking account of the high accuracy of

the instrument used (±0.0001 m^2/g), the surface area values were rounded to whole numbers, and the mean pore size (S_p) and total pore volume (V_p) calculated using the BJH algorithm were rounded to one and two decimal places respectively.

3 Results and discussion

3.1 Chemical composition of powder materials

After leaching the powder material in a solution of HCl:H_2O it was possible to determine the mass content of silica, and using AAS analysis—quantitative determination of Mg^{2+} (Table 1). Additionally, for precise determination of the composition of the obtained powder materials, the moisture content was determined (drying at 105 °C for 2 h). In the course of analyzes, it was found that the powders obtained via sol–gel process have similar moisture content, which is in the range of 10.1–13.6 %. Small differences in the moisture content of samples are related to the methods of their preparation (variants I–III) and the mass ratio of the used reagents. The remaining solid after the leaching process was dried and weighed to determine the amount of SiO_2 in the analyzed samples. The silica content in the obtained materials is in the range of 54.6–63.1 %, and is higher for the samples of $xMgO{\cdot}ySiO_2$ obtained using TEOS excess in relation to magnesium ethoxide, regardless the variant of the synthesis. However, the most important was precise quantitative determination of the magnesium content as a component of the $xMgO{\cdot}ySiO_2$ powder. For this purpose, filtrate after leaching of the initial material was used, which in principle should contain $MgCl_2$. AAS analysis results clearly confirmed the presence of magnesium in the tested samples which quantity, similarly as in the case of SiO_2, is determined by the mass ratio of TEOS:magnesium ethoxide.

Definitely a higher content of magnesium have samples MP 2.1–2.3 and MP 4.1–4.3, obtained using the same amount of organic precursors of the individual components of the $xMgO{\cdot}ySiO_2$ powder (1,970–2,450 mg/dm^3 Mg^{2+} in the filtrate analyzed). Leaching and quantitative analysis of the sample MP2.2, subjected to further detailed physicochemical analysis, proved the presence of 57.7 % of SiO_2 and 39.2 % of MgO (2,060 mg/dm^3 Mg^{2+} calculated into MgO present in 0.875 g of the sample subjected to leaching, considering the moisture, which is 12.5 %) which correspond to the powder formulae of $0.85MgO{\cdot}0.96SiO_2$. In turn, the quantitative analysis of the sample MP 1.2 has confirmed that it consists of 57.8 % of SiO_2 and 28.9 % of MgO related with formulae of $0.63MgO{\cdot}0.96SiO_2$ (1,520 mg/dm^3 Mg^{2+} calculated into MgO present in 0.873 g of the sample subjected to leaching, considering the moisture, which is 12.7 %), which proves earlier drawn conclusions regarding lower magnesium content in the samples obtained using an excess of TEOS. The quite similar content of silica, which should be also determined by the weight ratio of TEOS:magnesium ethoxide, is probably related with alkaline character of sol–gel synthesis (NH_3 catalyst) and relatively small excess of TEOS in respect to Mg precursor. In the case of higher excess of silica precursor as well as using acid catalyst, significant differences should be expected due to the changes in the hydrolysis and condensation rate determined by catalyst type. Preparation of $xMgO{\cdot}ySiO_2$ powder via sol–gel method in the presence of HCl catalyst is future stage of the research.

Quantitative analysis of the samples subjected to calcination process, including sample MP 2.2C, revealed that the moisture content does not exceed 1 %, and therefore the content of MgO and SiO_2 is slightly different, so these results are not presented in Table 1. Analysis of the composition of the samples MP 1.2C and MP 2.2C revealed that they consist of 63.4 % of SiO_2 and 26.8 % of MgO ($0.57MgO{\cdot}1.05SiO_2$), 62.3 % of SiO_2 and 36.9 % of MgO ($0.82MgO{\cdot}1.04SiO_2$), respectively.

In order to confirm the chemical composition of the $xMgO{\cdot}ySiO_2$ powders, energy dispersive X-ray microanalysis (EDS) was performed. The main aim of EDS was to confirm the presence of magnesium, silicon and oxygen, which should be a part of the synthetic powders taking into account the type of reactants used for its synthesis, and also to determine the impact of the basic process parameters on the quality of the products obtained. The results of EDS analysis are summarized in Table 1; they represent the content of each element (percent mass contribution) in the structure of the $xMgO{\cdot}ySiO_2$. Additionally, to confirm the presence of Si–O–Mg bonds in tested $xMgO{\cdot}ySiO_2$ powder, XPS analysis was performed. Detailed results in comparison with selected reference samples are presented as supplementary materials (see supplementary data – Figs. S1-S3 and Table S1).

It was found that the contributions of individual elements are dependent on the order of dosing of the silicon precursor and catalyst, as well as the mass ratio of the two reactants. Moreover, it was observed that samples MP 1.1 and MP 3.1 (synthesized with the quantity of NH_4OH reduced by half) have comparable mass contributions from magnesium, silicon, and oxygen. These samples were obtained by introducing into the reaction system (magnesium ethoxide) first a 25 % ammonia solution, and then TEOS. On the basis of the percentage mass contribution of each element, the oxide composition of the samples was determined; for sample MP 1.1 it was 36.2 % MgO and 63.8 % SiO_2 ($0.75MgO{\cdot}1.06SiO_2$), while for sample MP 3.1 it was 38.1 % MgO and 61.9 % SiO_2 ($0.57MgO{\cdot}1.05SiO_2$).

Table 2 Composition of $xMgO{\cdot}ySiO_2$ powders including average results from AAS analysis, gravimetric method and EDS technique for each stoichiometry

$xMgO{\cdot}ySiO_2$	AAS and gravimetric analysis	
	Samples MP 1.1–1.3 TEOS:magnesium ethoxide:NH_4OH mass ratio 1.5:1:0.5	Samples MP 2.1–2.3 TEOS:magnesium ethoxide:NH_4OH mass ratio 1:1:0.5
x	0.64	0.89
y	0.99	0.95
	Samples MP 3.1–3.3 TEOS:magnesium ethoxide:NH_4OH mass ratio 1.5:1:0.25	Samples MP 4.1–4.3 TEOS:magnesium ethoxide:NH_4OH mass ratio 1:1:0.25
x	0.71	0.94
y	0.99	0.95
$xMgO{\cdot}ySiO_2$	EDS analysis	
	Samples MP 1.1–1.3	Samples MP 2.1–2.3
x	0.69	0.96
y	1.00	0.83
	Samples MP 3.1–3.3	Samples MP 4.1–4.3
x	0.81	0.99
y	1.00	0.85

A similar composition was found for samples MP 2.3 and MP 4.3 (also synthesized with the quantity of basic catalyst reduced by half), in which the percentage mass contribution of magnesium is ca. 22 % and that of oxygen ca. 52 %. In all of the above-mentioned powders the mass contribution of magnesium is more than 20 %, that of oxygen is more than 50 %, and that of silicon is nearly 30 %. An exception is sample MP 2.1, in which the percentage mass contribution of silicon is only 18 %. This sample was prepared by introducing catalyst and TEOS sequentially into the reaction system. In the case of samples obtained at a TEOS to magnesium precursor ratio of 1.5:1, the experimental data indicate a greater mass contribution of each element constituting the material as compared with the other samples.

The EDS analysis proves the presence of typical elements characteristic for $xMgO{\cdot}ySiO_2$ powder synthesized via sol–gel method. The percentage mass contributions of each element constituting the material are quite high, considering that when $xMgO{\cdot}ySiO_2$ is obtained in an aqueous system the MgO content is <20 %, SiO_2 <65 %, and the moisture is 18 % [31], resulting in the more hydrophilic nature of the synthetic powders obtained. In the case of the materials prepared via the sol–gel method, the moisture content is negligible, as a result of the synthesis methodology. In addition, powders subjected to calcination are completely free of moisture, resulting only in a minor change in the percentage contribution of oxygen in the structure of the powders, observed during the EDS analysis, and not presented in Table 1. Additionally, a change in the mass ratio of $MgO:SiO_2$ in the final product significantly influences the physicochemical properties of the $xMgO{\cdot}ySiO_2$, in the order of emphasizing the properties of MgO or SiO_2. Those results correspond to the dependencies obtained during AAS analysis.

Table 2 presents the composition of $xMgO{\cdot}ySiO_2$ powders based on average results from AAS analysis, gravimetric method and EDS technique for each stoichiometry. It was found that this composition is mainly determined by the mass ratio of reactants used, especially excess of TEOS which results in smaller contribution of MgO in synthesized powder. AAS as well as gravimetric analysis proved that $xMgO{\cdot}ySiO_2$ can be consider as $0.64MgO{\cdot}0.99SiO_2$ or $0.71MgO{\cdot}0.99SiO_2$, when powders were synthesized using TEOS:magnesium ethoxide mass ratio of 1.5:1, and as $0.89MgO{\cdot}0.95SiO_2$ or $0.94MgO{\cdot}0.95SiO_2$, when powders were synthesized using TEOS:magnesium ethoxide mass ratio of 1:1. Slightly different results were obtained during EDS analysis which is rather qualitative in respect to AAS, but they also confirms the influence of mass ratio of reactants on the composition of final powder.

3.2 Crystalline structure

Selected samples of $xMgO{\cdot}ySiO_2$ were tested to determine the crystalline structure. The most important results of the analysis are shown in Fig. 2. The prepared samples of $xMgO{\cdot}ySiO_2$ powder (samples MP 1.2 and MP 2.2) not subjected to calcination are completely amorphous (Fig. 2a, b). During the study it was found that calcination of these powders at 1,000 °C leads to the formation of clinoenstatite—a crystalline variety of $MgSiO_3$ (Fig. 2c)—and forsterite—a crystalline variety of Mg_2SiO_4 (Fig. 2d). This is evidenced by the characteristic diffraction bands at 2Θ values of 28, 30, 31, 38 and 58 (clinoenstatite) and 18, 23, 24, 26, 30, 32, 35, 36, 38, 39, 52, 62, 63 (forsterite). It should be noted that by reducing the amount of TEOS in the preparation of powders MP 2.1C–2.3C, as compared with materials MP 1.1C–1.3C, different crystalline forms after calcinations were obtained, demonstrating the ability to control the structure of these type of powders obtained in the sol–gel process. Moreover, the crystalline structure of such powders determines potential routes for their use. Additionally, it was confirmed that changing the order in which the reactants were introduced into the reaction system (variants I–III, samples MP 1.1C–1.3C or MP 2.1C–2.3C), or changing the quantity of catalyst introduced in the

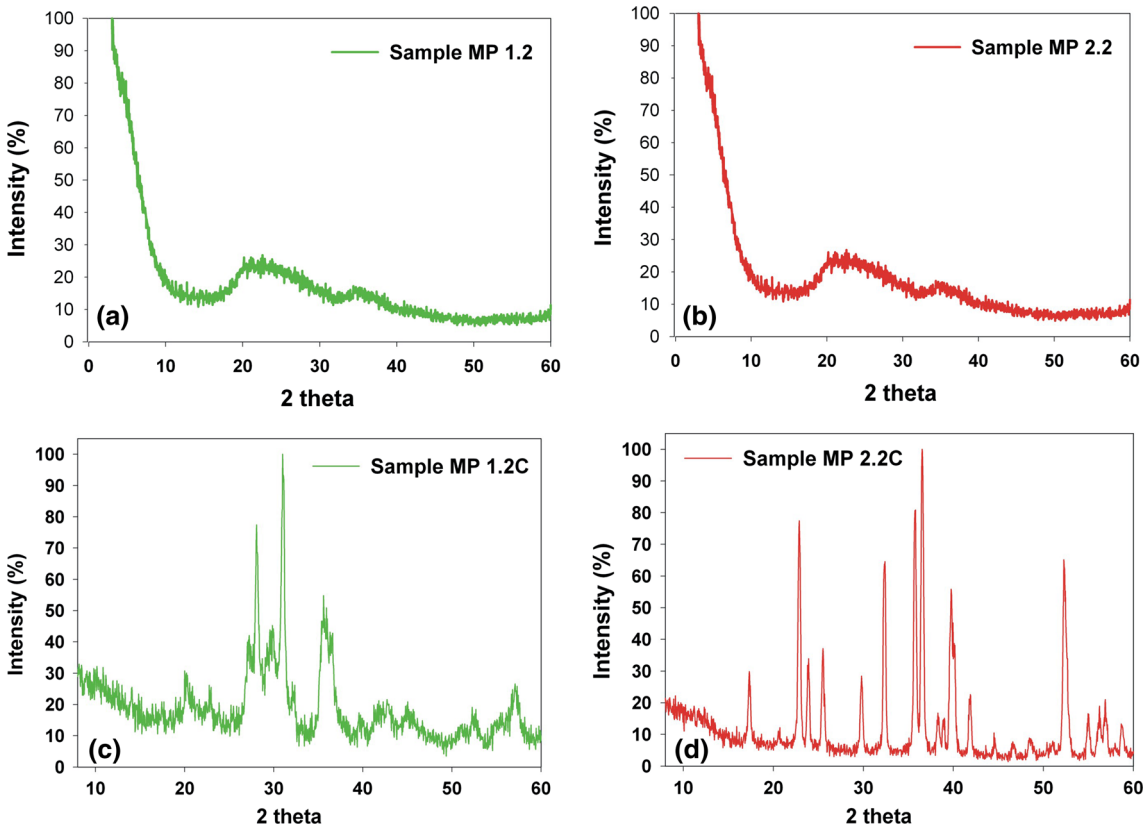

Fig. 2 WAXS patterns of $xMgO{\cdot}ySiO_2$ powders obtained via the sol–gel method using different mass ratio of TEOS:magnesium ethoxide:NH_4OH: **a** 1.5:1:0.5 and **b** 1:1:0.5 without calcination, and **c** 1.5:1:0.5 and **d** 1:1:0.5 additionally calcined at 1,000 °C for 2 h

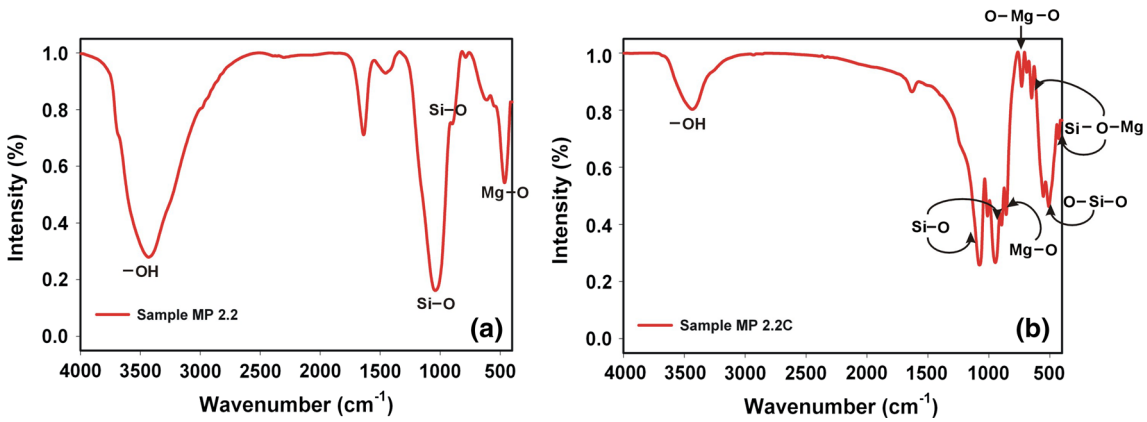

Fig. 3 FT-IR spectra of non-calcined and calcined $xMgO{\cdot}ySiO_2$ powders

case of samples MP 3.1C–3.3C and 4.1C–4.3C, does not generate additional changes in the crystalline structure of the resulting, calcined powder materials, hence the WAXS patterns of other systems are not shown. Detailed XRD investigations, in comparison with selected reference samples, are presented as supplementary materials (see supplementary data – Fig. S4).

3.3 FT-IR analysis

In order to confirm the results of WAXS analysis, and indirectly, the efficiency of the preparation of $xMgO{\cdot}ySiO_2$ powder FT-IR spectra of the sample MP 2.2 and its calcined form MP 2.2C were analyzed. Talc was used as reference sample and its FT-IR spectrum is presented in

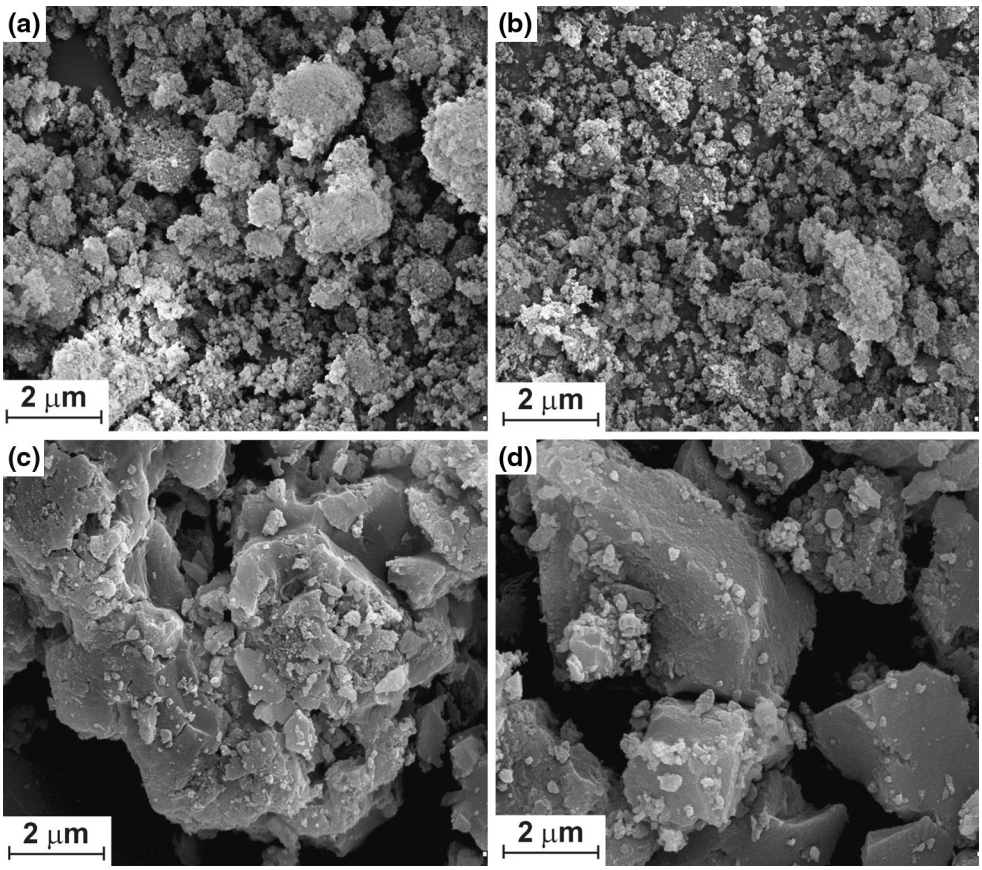

Fig. 4 SEM images of $xMgO{\cdot}ySiO_2$ powders obtained via the sol–gel method using different mass ratio of TEOS:magnesium ethoxide:NH_4OH: **a** 1.5:1:0.5 and **b** 1:1:0.5 without calcination, and **c** 1.5:1:0.5 and **d** 1:1:0.5 additionally calcined at 1,000 °C for 2 h

Fig. S5. The FT-IR spectrum of the sample MP 2.2 (Fig. 3a) shows the signals characteristic for $xMgO{\cdot}ySiO_2$ powder not subjected to calcination. A clear, broad signal at a wavenumber 3,650–3,350 cm^{-1} is generated by the stretching vibration of hydroxyl groups. In turn, the band with significant intensity, with a maximum at a wavenumber of about 1,050 cm^{-1} is characteristic for the stretching vibration of Si–O [32]. Visible is also a clear signal at 480 cm^{-1}, originating from the deformation vibration of Mg–O bonds. The presence of other bands specific for the groups of analyzed product is somewhat masked by the presence of significant quantities of water in its structure, which can be confirmed by a signal appearing at 1,630 cm^{-1} related with a bending vibrations derived from water molecules that have been physically adsorbed on the surface of the resulting powder.

Slightly more legible is the FT-IR spectrum of the sample subjected to the calcination process (MP 2.2C) in which the amount of water has been drastically reduced. Results of FT-IR analysis of this sample show the presence of signals characteristic for the $xMgO{\cdot}ySiO_2$ powder with a defined structure of forsterite, and so for the material of the chemical formula Mg_2SiO_4. Similar to the spectrum of the compound before calcination, there is a visible signal characteristic for –OH groups, but it has a much lower intensity. In the range of 1,100–500 cm^{-1} there is numerous of visible signals which evidence a formation of powder. The signals appearing at wavenumbers of 1,100 and 890 cm^{-1} derived from stretching and deformation vibrations of Si–O groups [33, 34]. Moreover, visible is a signal with a maximum intensity at a wavenumber of 630 cm^{-1}, which comes from the deformation vibrations of O–Mg–O bonds. However, the most important signals, which confirm receipt of $xMgO{\cdot}ySiO_2$ powder, are those at wavenumbers of 428 cm^{-1} and about 645 cm^{-1}. Those bands are characteristic for the deformation vibration of Si–O–Mg, which evidence the formation of specific chemical species. At the wavenumber of 538 cm^{-1} there is a clear band, derived from stretching vibration of Si–O–Si bonds, that are present in the structure of the analyzed material [28]. In turn, a signal at 1,630 cm^{-1}, related with a bending vibrations, is derived from water molecules that have been physically adsorbed on the surface of the resulting powder. However, this signal is characterized by a considerably lower intensity than in the case of uncalcined sample. The results confirm earlier drew conclusions

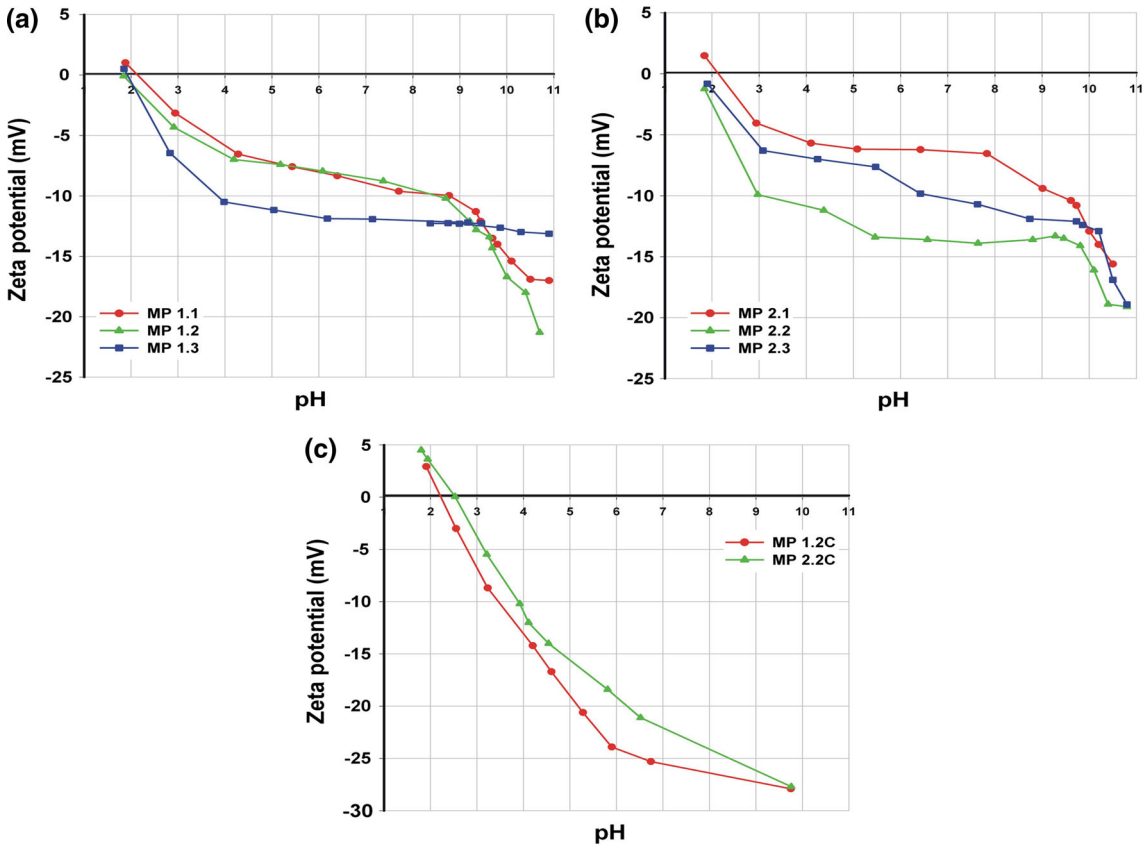

Fig. 5 Zeta potential versus pH for $xMgO{\cdot}ySiO_2$ powders obtained using a TEOS:magnesium ethoxide:NH_4OH mass ratio of **a** 1.5:1:0.5 and **b** 1:1:0.5 without calcination, and **c** 1.5:1:0.5 and 1:1:0.5 additionally calcined at 1,000 °C

on the efficient of production of $xMgO{\cdot}ySiO_2$ powder based on a sol–gel method.

3.4 Dispersion and morphology of $xMgO{\cdot}ySiO_2$ powders

A study of the $xMgO{\cdot}ySiO_2$ powders obtained via the sol–gel method enabled a careful analysis of their dispersion characteristics and morphology. For this purpose, the samples were observed using a scanning electron microscope, the SEM images being presented in Fig. 4.

The surface morphology and nature of the dispersion of the produced powders are very similar. The SEM images in Fig. 4a, b show samples MP 1.2 and 2.2, which were obtained at different reactants mass ratios, but were not subjected to the calcination process. The particles in these samples exhibit substantial homogeneity, and their average size is less than 10 μm. Another very important fact is their tendency to form spherical structures. A slightly better surface morphology was found for sample MP 2.2 (Fig. 4b), indicating that the mass ratio of the reactants has a significant effect on the nature of the dispersion of the powders. In the course of further tests, the method of preparation of $xMgO{\cdot}ySiO_2$ was also found to have a significant impact on the size and shape of the particles. It was found that the best-formed, homogeneous materials were obtained in process variant II (when the SiO_2 precursor and the catalyst NH_4OH were introduced simultaneously into the system). Tests of the same powders (MP 1.2C and 2.2C) additionally calcined at 1,000 °C showed that the process of heat treatment resulted in significant changes in the morphology of the particles. The analyzed materials are characterized by the presence of particles having irregular shapes. The presented SEM images confirm that particles of the powders have a tendency to form aggregates and agglomerate structures, and thus cause an increase in the basic dispersive parameters, such as their diameter. This is the result of the baking of individual particles and closure of their pores due to the sudden removal of the moisture present in the samples after the precipitation process, and also the formation of a compact and dense crystalline structure, as confirmed by the images in Fig. 4c, d.

An important factor leading to noticeable changes in the dispersion and morphology characteristics was the reduction by one half in the amount of catalyst (NH_4OH) used in preparing the $xMgO{\cdot}ySiO_2$ systems labeled as MP 3.1–3.3 and 4.1–4.3. Again there was found to be an increase in the

Table 3 Parameters of the porous structure of $xMgO{\cdot}ySiO_2$ powders produced via sol–gel method

Sample symbol	Surface area (m^2/g)	Total volume of pores (cm^3/g)	Mean diameter of pores (nm)
Without calcination			
MP 1.1	515	0.34	2.6
MP 1.2	568	0.38	2.7
MP 1.3	425	0.30	2.6
MP 2.1	410	0.32	2.5
MP 2.2	431	0.30	2.6
MP 2.3	391	0.30	2.4
Calcined at 1,000 °C			
MP 1.1C	0.8	0.0003	4.2
MP 1.2C	2.3	0.0004	4.4
MP 1.3C	0.5	0.0003	4.2
MP 2.1C	0.6	0.0003	3.9
MP 2.2C	1.4	0.0004	4.1
MP 2.3C	0.7	0.0003	4.0

heterogeneity of the samples, and thus in the tendency of particles to form agglomerate structures.

Based on the tests performed it was found that the factor most significantly influencing the dispersion characteristics and morphology of the powders obtained via the sol–gel process is the order in which the reactants are introduced (variants I–III). Undoubtedly the best morphology is exhibited by $xMgO{\cdot}ySiO_2$ samples obtained by means of simultaneous dosing of TEOS and basic catalyst into the reaction system (variant II).

3.5 Electrokinetic stability

The next step in the physicochemical analysis was to study the changes of zeta potential (ζ) versus pH (Fig. 5).

The electrokinetic curves of samples MP 1.1–1.3 (Fig. 5a) are very similar. In the pH range 2–11 all samples have negative zeta potential values. Small differences in the course taken by the electrokinetic curves of the samples are related to the method of preparation, which in this case, as it turns out, does not play a significant role. This is confirmed by the small differences in the values of the isoelectric point (IEP) of the powders: for sample MP 1.1 the value is 2.1, and for sample MP 1.3 it is 1.9. The most negative value of the zeta potential (−21.3 mV) was recorded for sample MP 1.2. The materials have their greatest electrokinetic stability at pH $\geq$ 10, which is an important factor in their possible applications.

Changing the mass ratio of the reactants (TEOS:magnesium ethoxide) to 1:1 resulted in significant changes in the electrokinetic properties of samples MP 2.1–2.3 (Fig. 5b). All samples also had negative zeta potential values in the analyzed pH range. Only sample MP 2.1 exhibited an IEP, at pH = 2.1. In this group of samples, the most negative electrokinetic potential value (−19.0 mV) was recorded for samples MP 2.2 and MP 2.3. Samples MP 2.1–2.3 were again found to have their highest electrokinetic stability at pH $\geq$ 10.

The process of additional calcination of the precipitated powders caused significant changes in their electrokinetic characteristics. Similarly as with the formation of a stable crystalline structure, calcination resulted in a significant increase in the electrokinetic stability of the resulting products (Fig. 5c), evidenced by the significantly higher values of zeta potential at selected pH values for non-calcined systems. A noteworthy fact is the stability of the electrokinetic curves, which in the case of samples MP 1.2C and 2.2C do not contain significant bends, and reached IEPs at 2.24 and 2.55 respectively.

Evaluation of the electrokinetic properties clearly confirmed that this parameter is especially influenced by the mass ratio of the reactants. Changing the order of dosing of the reagents in this case does not affect the electrokinetic properties of the resulting systems.

3.6 Parameters of porous structure

Characteristics of the porous structure plays an important role in application of this type of materials as supports for selected organic and inorganic substances, on the other hand as adsorbents. Table 3 shows the basic parameters of the porous structure of the $xMgO{\cdot}ySiO_2$ powders obtained using the sol–gel method.

Analysis of these data clearly demonstrates the effectiveness of the sol–gel process for the preparation of active $xMgO{\cdot}ySiO_2$ powders. For all samples, high values of surface area were obtained. The highest value (A_{BET} = 568 m^2/g) was measured for sample MP 1.2, obtained with a TEOS:magnesium precursor:NH_4OH mass ratio of 1.5:1:0.5 and with simultaneous dosing of silicon precursor and catalyst (NH_4OH). Slightly lower surface area values were found for samples MP 1.1 (A_{BET} = 515 m^2/g) and MP 1.3 (A_{BET} = 425 m^2/g), which clearly indicates the significant effect of the order of dosing of TEOS and catalyst to the reaction system. Reducing the quantity of TEOS used in the sol–gel process led to products of lower activity than samples MP 1.1–1.3. In this group of samples the highest surface area value was examined for sample MP 2.2 (A_{BET} = 431 m^2/g). The values for pore volume and diameter were similar for all of the precipitated powders (V_p = 0.30–0.38 cm^3/g and S_p = 2.4–2.7 nm). The calcination process performed on selected samples caused significant changes in the porous structure parameters. In particular, there was a significant reduction in the surface area and pore volume for the

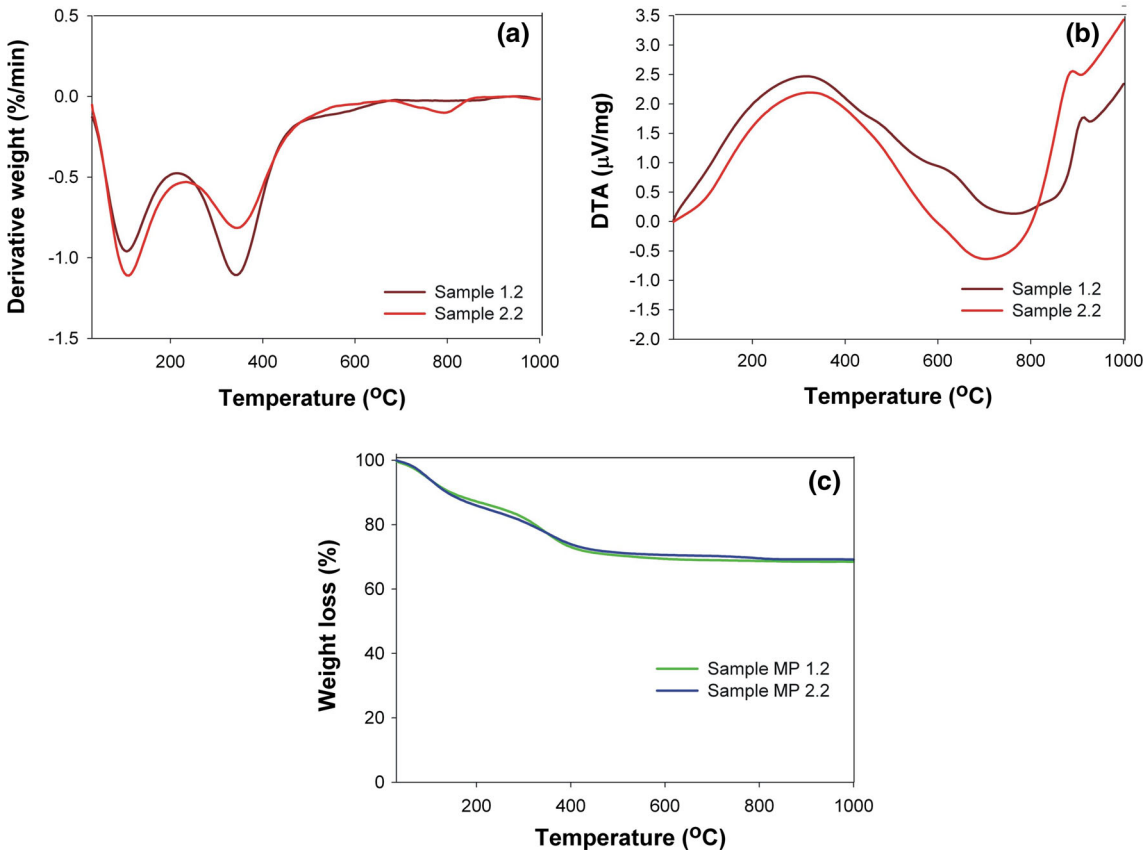

Fig. 6 Thermograms of $xMgO{\cdot}ySiO_2$ powders obtained via the sol–gel method: **a** DTG, **b** DTA and **c** TG curves

calcined samples. The highest surface area values in this group of samples were estimated for the materials MP 1.2C (2.3 m^2/g) and MP 2.2C (1.4 m^2/g). The pore volume of these powders is in the range 0.0003–0.0004 cm^3/g. There was also found to be a somewhat larger pore diameter, which in the case of the calcined samples ranged from 3.9 to 4.4 nm. Such significant changes in the porous structure parameters are most likely related to structural changes of particles of the powders subjected to the process of calcination, and unambiguously confirm the conclusions drawn from the analysis of SEM images. The above experimental data showed that the best porous structure parameters are obtained for the hybrid materials obtained via variant II of the preparation process, irrespective of the mass ratio of the reactants.

3.7 Thermal stability

The thermal stability of the hybrid materials obtained without calcination was determined by means of thermal analysis. Thermogravimetric curves (TG), as well as their first derivatives (DTG and DTA), were obtained (Fig. 6).

The thermogravimetric curves for the $xMgO{\cdot}ySiO_2$ powders shown in Fig. 6c indicate a three-stage mass change. Loss of mass of the powders was found to begin even at the starting temperature of 30 °C, and the observed mass loss over the temperature range 30–200 °C is relatively large, at around 11 %. This is also indicated by the clear peak appearing on the derivative curve (Fig. 6a). The second stage, with a mass loss of approximately 20 % over the temperature range 200–600 °C, also involves chiefly the local elimination of water present in the powders structure. The significant change in mass is confirmed by the sharp peak on the DTG curve (Fig. 6a), with a maximum at approximately 380 °C for both hybrid materials (MP 1.2 and 2.2). By way of further confirmation the DTA curve is presented (Fig. 6b), which shows peaks in the temperature range 30–200 °C related to the endothermic effect of the samples' dehydration, and in the range 200–600 °C related to an exothermic thermal effect. Thermal processing above 600 °C (up to 1,000 °C) in the third stage causes a gradual loss of mass by a further 2 % (above 800 °C), caused by the formation of new bonds as a result of the formation of clinoenstatite and forsterite—the crystalline structures of samples MP 1.2 and 2.2 respectively. These changes are well visible on the DTA curve, and are related to exothermic peaks near 850 °C—the temperature at which the crystalline form of $xMgO{\cdot}ySiO_2$

appears. The $xMgO{\cdot}ySiO_2$ powders were found to lose only 33 % of their total mass, which confirms their fairly high thermal stability. Insignificant differences in thermal stability, observed between samples MP 1.2 and 2.2 especially on the DTA and DTG curves, are related only to the quantities of reagents used for their preparation (the method of preparation was the same). The samples which had been calcined (at 1,000 °C) were not analyzed, in view of their thermal treatment method, well-formed crystalline structure and expected high thermal stability.

The results of research clearly confirmed the opportunities offered by the sol–gel method for the synthesis of such inorganic powders. On the one hand the impact of various process parameters on the properties of the resulting product was confirmed, on the other hand a new type of inorganic material with specific properties and possible a wide range of application (cheap polymer fillers or adsorbents) was obtained. Additional calcination process allows to form a particular crystalline structure which in some industries plays an important role, the same as in the case of the cited powder containing TiO_2 in its structure. Therefore, the spectrum of the synthesized compounds, based on a sol–gel process, can be effectively extended by $xMgO{\cdot}ySiO_2$ powder with defined physicochemical and structural properties.

4 Conclusions

The proposed method for the synthesis of $xMgO{\cdot}ySiO_2$ powders via a sol–gel process has made it possible to obtain valuable hybrid materials with specific properties. It was confirmed that the physicochemical properties of the materials produced are strongly dependent on the quantity of reagents and the methodology used for their preparation. It was shown that it is possible to design materials with defined dispersion parameters by controlling the mass ratio of the reactants and the order of their introduction into the reaction system. $xMgO{\cdot}ySiO_2$ samples obtained through simultaneous dosing of TEOS and basic catalyst into the reaction system (variant II) unquestionably exhibit the best morphology.

The AAS and EDS analyses proved the presence of typical elements characteristic for $xMgO{\cdot}ySiO_2$ powder synthesized via sol–gel method, as confirmed by the high content of magnesium and silicon (calculated to MgO and SiO_2 content respectively) in the structure of the product. In addition, it was confirmed that by changing the mass ratio of the precursors of the various elements we can control their content in the final product. The results also show that a product with an appropriate crystalline structure can be formed by means of an additional final treatment process such as calcination. Such technological operations may further increase the range of application of this type of materials.

The sol–gel process has proved to be very effective in the synthesis of active $xMgO{\cdot}ySiO_2$ powders, as is evidenced by the products' very high surface areas. In addition it was confirmed that, depending on needs, the parameters of the porous structure may also be controlled by selecting the ratio of the reactants, method of preparation, or method of final treatment (calcination).

Similarly to other physicochemical parameters, the electrokinetic properties and thermal stability are strongly influenced by the mass ratio of the reactants and the final calcination process. The resulting $xMgO{\cdot}ySiO_2$ powders offer high thermal and electrokinetic stability, especially at alkaline pH.

In view of the unique properties of the hybrid materials obtained, they will continue to be studied in a further stage of the research, which will deal with their application in various areas of technology.

Acknowledgments The study was financed within the Polish National Centre of Science funds according to Decision No. DEC-2011/03/D/ST5/05802.

References

1. Mastuli MS, Rusdi R, Mahat AM, Saat N, Kamarulzaman N (2012) Sol–gel synthesis of highly stable nano sized MgO from magnesium oxalate dihydrate. Adv Mater Res 545:137–142
2. Hench LL, West JK (1990) The sol–gel process. Chem Rev 90:33–72
3. Tamon H, Kitamura T, Okazak M (1998) Preparation of silica aerogel from TEOS. J Colloid Interface Sci 197:197–353
4. Kimura I, Taguchi Y, Tanaka M (1999) Preparation of silica particles by sol–gel process in reverse suspension. J Mater Sci 34:1471–1475
5. Kamitani K, Uo M, Inoue H, Makishima A (1993) Synthesis and spectroscopy of TPPS-doped silica gels by the sol–gel process. J Sol–Gel Sci Technol 1:85–92
6. Brambilla R, Radtke C (2010) Silica–magnesia mixed oxides prepared by a modified Stöber route: structural and textural aspects. Powder Technol 198:337–346
7. Brambilla R, Radtke C (2009) An investigation on structure and texture of silica–magnesia xerogels. J Sol–Gel Sci Technol 249:70–77
8. Sokolnicki J, Radzki S (2004) Spectroscopic behavior of hybrid materials obtained by the sol–gel technique. Opt Mater 26:199–206
9. Samuneva B, Kalimanova S, Kashchieva E (2003) Composite glass–ceramics in the systems $MgO–SiO_2$, $MgO–Al_2O_3–SiO_2$ and fluorapatite obtained by sol–gel technology. J Sol–Gel Sci Technol 26:273–278
10. Gross S, Müller K (2011) Sol–gel derived silica-based organic–inorganic hybrid materials as, composite precursors" for the

synthesis of highly homogeneous nanostructured mixed oxides: an overview. J Sol–Gel Sci Technol 60:283–298
11. Marcelo M, Tarik DS, Mohallem GLT (2006) Nanocrystalline titanium oxide thin films prepared by sol–gel process. Braz J Phys 3:1081–1083
12. Uhlmann DR, Teowee G, Boulton J (1997) The future of sol–gel science and technology. J Sol–Gel Sci Technol 8:1083–1091
13. Seck EI, Doña-Rodríguez JM, Pulido Melián E, Fernández-Rodríguez C, González-Díaz OM, Portillo-Carrizo D, Pérez-Peña J (2013) Comparative study of nanocrystalline titanium dioxide obtained through sol–gel and sol–gel–hydrothermal synthesis. J Colloid Interface Sci 400:31–40
14. Yan P, Jiang H, Zang S, Li J, Wang Q, Wang Q (2013) Sol–solvothermal preparation and characterization of (Yb, N)-codoped anatase-TiO_2 nano-photocatalyst with high visible light activity. Mater Chem Phys 139:1014–1022
15. Singhal A, Pai MR, Rao R, Pillai KT, Lieberwirth I, Tyagi AK (2013) Copper(I) oxide nanocrystals—one step synthesis, characterization, formation mechanism, and photocatalytic properties. Eur J Inorg Chem 14:2640–2651
16. Kesmez Ö, Burunkaya E, Asiltürk NM, Arpaç E (2011) Effect of acid, water and alcohol ratios on sol–gel preparation of antireflective amorphous SiO_2 coatings. J Non-Cryst Solids 357: 3130–3135
17. Lopez T, Garcia-Cruz I, Gomez R (1991) Synthesis of magnesium oxide by the sol–gel method: effect of the pH on the surface hydroxylation. J Catal 127:75–85
18. Rahmana IA, Vejayakumaran P (2007) An optimized sol–gel synthesis of stable primary equivalent silica particles. Colloids Surf A 294:102–110
19. Canbay CA, Aydogdu A (2009) Microstructure electrical and optical characterization of ZnO–NiO–SiO_2 nanocomposite synthesized by sol–gel technique. Turk J Sci Technol 4:121–125
20. Ibrahim IAM, Zikry AAF, Sharaf MA (2010) Preparation of spherical silica nanoparticles: Stöber silica. J Am Sci 6:985–988
21. Balachandaran K (2010) Synthesis of nano TiO_2–SiO_2 composite using sol–gel method: effect on size, surface morphology and thermal stability. Int J Eng Sci Technol 2:3695–3700
22. Sanosha KP, Balakrishnana A, Francisc L, Kima TN (2010) Sol–gel syntesis of forsterite nanopowders with barrow particle size distribution. J Alloy Compd 495:113–115
23. Mehta M, Mukhopadhyay M, Christian R, Mistry N (2012) Synthesis and characterization of MgO nanocrystals using strong and weak bases. Powder Technol 226:213–221
24. Bokhimi Morales A, Lopez T, Gomez R (1995) Crystalline structure of MgO prepared by the sol–gel technique with different hydrolysis catalysts. J Solid State Chem 115:411–415
25. Naghiu MA, Gorea M, Mutch E, Kristaly F, Tomoaia-Cotisel M (2013) Forsterite nanopowder: structural characterization and biocompatibility evaluation. J Mater Sci Technol 29:628–632
26. Chen XF, Li J, Feng TT, Jiang YS, Zhang XH, Wu HT, Yue YL (2013) Low-temperature synthesis of nano-crystalline $MgTi_2O_5$ powders by aqueous sol–gel process. Key Eng Mater 538: 177–180
27. Bayala N, Jeevanandam P (2012) Synthesis of NiO based bimetallic mixed metal oxide nanoparticles by sol–gel method. Adv Mater Res 585:164–168
28. Vishwas M, Narasimha Rao K, Arjuna Gowda KV, Chakradhard RPS (2011) Optical, electrical and dielectric properties of TiO_2–SiO_2 films prepared by a cost effective sol–gel process. Spectrochim Acta A 83:614–617
29. Aguado J, van Grieken R, López-Muñoz MJ, Marugán J (2006) A comprehensive study of the synthesis, characterization and activity of TiO_2 and mixed TiO_2/SiO_2 photocatalysts. Appl Catal A 312:202–212
30. Jung KY, Park SB (2001) Effect of calcination temperature and addition of silica, zirconia, alumina on the photocatalytic activity of titania. Korean J Chem Eng 181:879–888
31. Ciesielczyk F, Bartczak P, Wieszczycka K, Siwińska-Stefańska K, Nowacka M, Jesionowski T (2013) Adsorption of Ni(II) from model solutions using co-precipitated inorganic oxides. Adsorption 19:423–434
32. Moscofian ASO, Pires CTGVMT, Vieira AP, Airoldi C (2012) Organofunctionalized magnesium phyllosilicates as mono- or bifunctional entities for industrial dyes removal. RSC Adv 2:3502–3511
33. Lan J, Lv J, Zhang W, Feng J, Liu Y, Wang Z, Zhao M (2012) Discrimation of types of thermal sensitive paper by characterization of the inorganic additives by Fourier Transform Infrared Microscopy, Confocal Raman Microscopy, and Scanning Electronic Microscope-Energy Dispersive Spectroscopy. Anal Lett 45:2763–2773
34. Chabrol K, Gressier M, Pebere N, Menu MJ, Martin F, Bonino JP, Marichal C, Brendle J (2010) Functionalization of synthetic talc-like phyllosilicates by alkoxyorganosilane grafting. J Mater Chem 20:9695–9706